DOI: 10.1002/chem.200601272

Phosphorescent Dyes for OLEDs

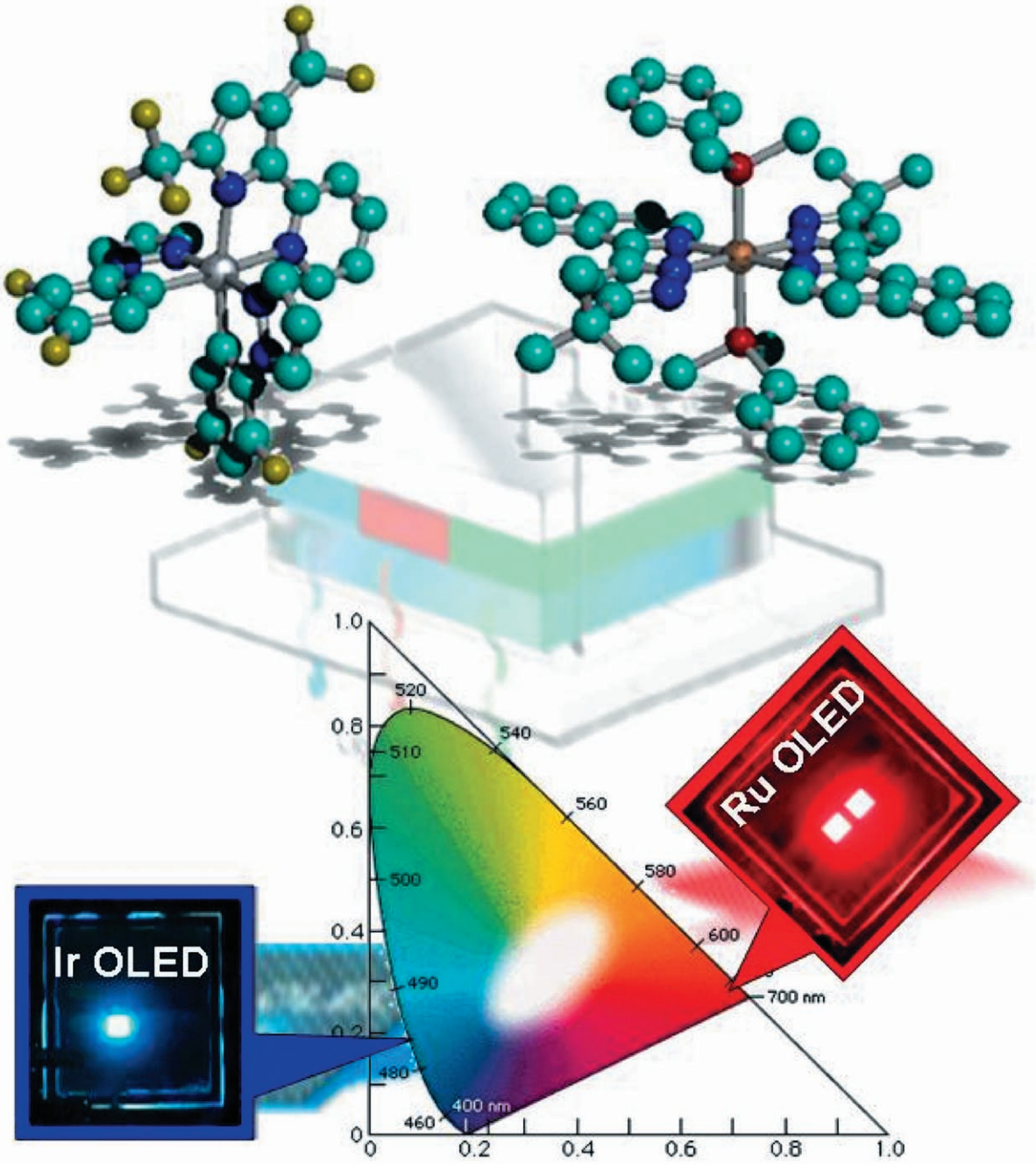

Phosphorescent Dyes for Organic Light-Emitting Diodes

Pi-Tai Chou*[a] and Yun Chi*[b]

Abstract: This article presents general concepts that have guided important developments in our recent research progress regarding room-temperature phosphorescent dyes and their potential applications. We first elaborate the theoretical background for emissive metal complexes and the strategic design of the chelating C-linked 2-pyridylazolate ligands, followed by their feasibility in functionalization and modification in an aim to fine-tune the chemical and photophysical properties. Subsequently, incorporation of 2-pyridylazolate chromophores is illustrated in the synthesis of the highly emissive, charge-neutral Os, Ru, Ir, and Pt complexes. Insights into their photophysical properties are gained from spectroscopy, relaxation dynamics, and theoretical approaches, from which the lowest-lying excited states, competitive radiative decay, and radiationless processes are then analyzed in detail. In view of applications, their potentials for OLEDs have been evaluated. The results, in combination with the fundamental basis, give a conceptual design contributed to the future advances in the field of OLEDs.

Keywords: iridium · N ligands · osmium · phosphorescence · platinum · ruthenium

Introduction

Second- and third-row transition-metal complexes incorporating chelating chromophores, such as 2,2′-bipyridine (bpy)[1] and 2-phenyl pyridine (ppy),[2] have attracted a great deal of study in recent years. Work focusing in this area was principally motivated by the use of these emissive complexes in the fundamental approaches of excited-state electron and energy transfer[3] as well as the potential applications in the fabrication of chemical and biological sensors, various photovoltaics, and organic light-emitting diodes (OLEDs).[4]

Recently, much attention has been paid to the preparation of this class of emissive materials with various types of ligands and to gain more understanding on their associated photophysical properties aimed at applications as OLEDs. In our approach, we recognized that the C-linked 2-pyridylazoles are akin to both 2,2′-bipyridine and 2-phenylpyridine, in that 2-pyridylazoles are capable of using two adjacent nitrogen atoms to form a stable chelate interaction.[5] Moreover, due to its strong acidity,[6] which is also reinforced in the case for R = electron withdrawing substituent such as CF_3, the azoles will readily lose a proton from the NH fragment, giving a stable anionic ligands. The strong σ-donor property of the azolate, together with the π-accepting ability of the second pyridyl fragment,[7] may provide a synergism of the electron delocalization so that the electron density is transferred from azolate to the metal ion and back to the pyridyl side of the ligand, thus enhancing the chelate interaction. Alternatively, the high acidity of the azolate N–H bonding would also allow a greater possibility for its insertion, normally under a kinetic control, to afford the third-

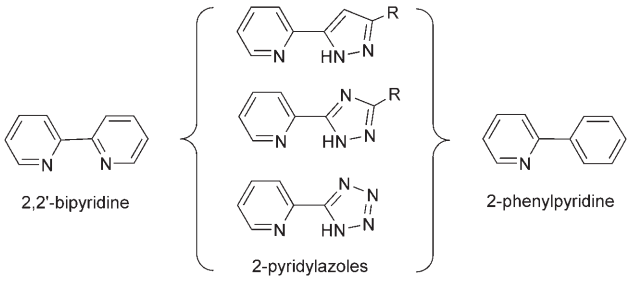

[a] Prof. P.-T. Chou
Department of Chemistry, National Taiwan University
No. 1, Section 4, Roosevelt Road, Taipei 10617 (Taiwan)
Fax: (+886) 2-2369-5208
E-mail: chop@ntu.edu.tw

[b] Prof. Y. Chi
Department of Chemistry, National Tsing Hua University
101, Section 2, Kuang Fu Road, Hsinchu 30013 (Taiwan)
Fax: (+886) 3-572-0864
E-mail: ychi@mx.nthu.edu.tw

row metal complexes, for which the 2-phenylpyridine type of ligand has failed to react properly, particularly for the less reactive Os^{II} system.

As for the metal center, the preparation of the isoelectronic transition-metal (Ru^{II}, Os^{II} and Ir^{III}) complexes that possess a unique d^6-electron configuration was found particularly attractive, because of their strong metal–ligand interaction and high luminescence efficiencies.[8] The strong spin–orbit coupling expected for these heavy-metal ions would lead to an efficient intersystem crossing from the singlet excited state to the triplet manifold. Furthermore, mixing singlet and triplet excited states through spin–orbit coupling, to a large extent, would partially remove the spin-forbidden nature of the $T_1 \rightarrow S_0$ radiative relaxation, resulting in the highly intense phosphorescent emission with a short radiative decay time (vide infra). Based on these concepts, the aforementioned diimine, cyclometalated as well as pyridylazolate chelating ligands can form rigid molecular frameworks with these heavy transition-metal ions and then give rise to the desirable absorption and efficient emission under optimum chemical modification. More specifically, these chelate complexes would display bright phosphorescent emission spanning the whole visible spectra, making them suitable to serve as ideal phosphors for OLED applications.

Theoretical Background

Emissive metal complexes maybe classified by various criteria such as the valence-electron configuration at the metal, the type of the electronic transitions, and the correlation among lower-lying electronic excited states. One review article has focused on sorting these materials according to the metal elements involved.[9] Like typical small organic fluorescent molecules, a great deal of the photochemical and physical behavior of luminescent metal complexes can be explained by the use of basic photophysics and molecular orbital theory.[10] It states that the electron density in each of the frontier molecular orbitals are not equally delocalized between metal and ancillary ligands, but preferentially located at the metal or the ligands. The electronic transition can be considered as the one-electron excitation that occurs among the associated frontier orbitals. This makes design and preparation of emissive metal complexes feasible if one can gain detailed understanding into the various factors that control these elemental photophysical properties. A brief summary on the nature of the electronically excited states commonly found in luminescent metal complexes is illustrated below:

Metal-centered (MC) excited states: Typical metal complexes with a partially filled d shell at the metal center are characterized by low-energy MC excitation states, which arise from electron hopping between the nonbonding (d_π) and antibonding (d_{σ^*}) orbitals. These d–d transitions are Laporte-forbidden, showing exceedingly low transition probability for the occurrence of both MC-based absorption and emission signals, although certain asymmetric, nonplanar vibrations may relax this restriction. Small splitting of the metal d orbitals is anticipated for the first-row transition-metal complexes due to the weak metal–ligand bonding, and promotion to the MC state often leads to facile ligand dissociation, because it possesses a significant amount of metal–ligand antibonding character. Due to its lower energy, population of the MC state may be thermally accessible, leading to the photodecomposition. For the second- and/or third-row transition-metal complexes with strong-field ligands in the spectrochemical series, the anticipated MC transitions are destabilized to the higher-energy region, such that the population to these states becomes less accessible. Accordingly, the interference of the MC states, that is, the quenching of the lowest-energy electronic transition, is significantly diminished. Finally, spin-selection rules are not strictly obeyed for these second- and third-row transition-metal complexes, for which the singlet-to-triplet intersystem crossing is facilitated by the heavy-atom enhanced spin–orbit coupling. As a consequence, many of them have exhibited highly efficient, room-temperature phosphorescence in both fluid and solid states.

Metal-to-ligand charge-transfer (MLCT) states: Metal-to-ligand charge-transfer (MLCT) states involve electronic transitions from a metal-based d orbital to a ligand-based delocalized π^* antibonding orbital.[11] In a conventional sense, the corresponding excitation results in metal oxidation and concomitant ligand reduction. These transitions are commonly observed in the middle- and late-transition-metal complexes possessing relatively low oxidation potentials. As a result, the reducing metal center renders the easily accessed d_π electrons, while the acceptor ligands, with π^* unoccupied orbitals at lower energies, accommodate the ejected electrons. Since the π^* ligand orbital is usually delocalized over the acceptor ligand, the population to MLCT states may only cause minimum structural distortion, facilitating its radiative recombination, decay process with remarkable efficiency.

The MLCT states of the first-row transition-metal complexes, in general, are quite reactive, but they become stable and highly luminescent upon shifting the metal to its second- and third-row counterparts, resulting from a systematical increase in metal-ligand bonding strengths, accompanied by destabilizing the aforementioned MC excited states, and consequently the reduction of the radiationless deactivation. Moreover, MLCT transitions are strongly allowed processes, manifested by intense absorption bands in the visible or near UV spectral regions, typical for a symmetry-allowed electronic transition. Irradiation into the MLCT states is thus a very efficient process to collect light energy. Likewise, emission generated from MLCT excited state may equally efficient in producing bright luminescence for various illumination applications.

Generally speaking, emissive MLCT states are observed for transition-metal complexes with d^6 and d^8 configurations. The versatility in molecular design makes possible a wider

selection for metal complexes that can undergo the MLCT excitation. For instance, all four W^0, Re^I, Os^{II}, and Ir^{III} metal elements would provide the anticipated d^6 electronic configurations. However, neutral diimine chromophores, such as bipyridine or phenanthroline, and π-accepting ancillary ligands, such as carbon monoxide, are essential in assembling and stabilizing the neutral tungsten complexes with formula $[W(CO)_4(diimine)]$.[12] The mechanistic studies on $[W(CO)_4(phen)]$ have shown a prototypical case of a slow, but measurable CO/Lewis base ligand substitution induced by the MLCT excitation, giving rise to an inferior stability of the W^0 complexes, due to a relative weak ligand-to-metal bond strength for the zero-valent metal center. In contrast, the relatively more stable Re^I–carbonyl complexes $[Re(CO)_3X(diimine)]$ (X = halides) and the corresponding derivatives have been successfully employed in fabrication of some OLEDs,[13] due to the stronger +1 charged metal–ligand bonding, albeit their with lower luminescence efficiency and longer emission wavelengths. Nevertheless, at current stage, it seems unlikely that the tungsten- and rhenium-incorporated emitters can be of significant value to serve as robust and long-lasting emitters for electroluminescent applications.

Intraligand (IL) ππ* excited states: Intraligand (IL) ππ* excited states originate from electronic transitions between π orbitals that are mainly localized on the ligand chromophore. As such, if the metal perturbation upon coordination is minimized, the luminescent complex may exhibit a transition that has spectral properties closely resembling the free ligand states. Accordingly, in view of the main-group metal elements such as Mg^{II}, Zn^{II}, Al^{III}, and their closed shell analogues that do not participate in the ππ* transitions of ligands, the observed emission from these metal complexes should be ascribed to the IL ππ* type. Based on this delineation, the identification of ππ* emission becomes straightforward. For example, the green-emitting $[AlQ_3]$ (Q = 8-quinolinate), its derivatives, and even the related white-emitting $[Zn(btz)_2]$ (btz = 2-(2-hydroxyphenyl)benzothiazolate)[14] were found to involve a substantially amount of IL ππ* character.

Ligand-to-metal charge-transfer (LMCT) excited states: Complexes with metal atoms in high oxidation states might show luminescence from ligand-to-metal charge-transfer (LMCT) states. These complexes typically constitute early transition-metal complexes with cyclopentadienyl or with simple σ-bonded anionic ligands. Representative complexes such as $[Ta(C_5Me_5)Cl_4]$ and $[Ta(NPh)Cl_3(L)_2]$ (L = donor ligand such as dimethoxyethane and pyridine) are known to exhibit room-temperature phosphorescence at the lower-energy region of visible spectra and with lower quantum efficiencies.[15] Other candidates that exhibit LMCT emission are a class of d^{10} complexes involving Cu^I, Ag^I, and Au^I metals; suitable examples are the tetrametallic Cu^I clusters as they exhibit bright phosphorescence.[16] OLED devices incorporating a similar class of Cu^I emitters have been fabricated;[17] however, none of them have shown performance data comparable to those fabricated using previously mentioned MLCT and/or IL ππ* emitting materials.

Effect of metal and state mixing: The above-mentioned four types of transition properties as well as the interactions among states with different characters play an important role in the intrinsic relaxation dynamics and consequently the luminescence efficiency. On one hand, except for the early transition-metal complexes, weakening of the metal–ligand bond strength is expected for MC and probably LMCT excitation, such that the resulting shallow potential-energy curve may intercept with the ground state, enhancing the radiationless deactivation. On the other hand, owing to the direct involvement of the d_π electron, spin–orbit coupling should be largely enhanced in the MLCT state of the heavy-metal complexes, manifesting its mixing properties between triplet and singlet manifolds. Consequently, the associated phosphorescence efficiency should increase due to its increasingly allowed transition probability. In sharp contrast to MLCT, due to its lack of direct incorporation with metal-center electron density, one thus expects much less singlet–triplet mixing in the IL ππ* state. As a result, the associated phosphorescence is subject to much longer radiative lifetime, such that any radiationless deactivation may cause the quench of the emission, resulting in low phosphorescence efficiency.

For transition-metal complexes with complicated molecular structures, the proximity in energy among several states is common. As for the first-order approximation, mixing among various transitions are natural and may play a central role for decent phosphorescence efficiency. A prototypical example illustrated here is the mixing between MLCT and LC ππ* electronic transitions, the result of which makes the fast singlet-to-triplet intersystem crossing feasible. Theoretically, for a simple $S_1 \rightarrow T_1$ intersystem crossing and vice versa, the corresponding rate constant, k_{isc}, is given by Equation (1) in which H_{so} is the Hamiltonian for the spin-orbit coupling and is the energy difference between the respective singlet and triplet states.

$$k_{isc} \propto \frac{|\langle T_1|H_{so}|S_1\rangle|^2}{(\Delta E_{S_1-T_1})^2} \quad (1)$$

As such, mixing of ππ* and MLCT characters in both S_1 and T_1 excited states leads to the incorporation of both and terms.[18] The net result is to induce the change of orbital angular momentums, namely the $d_\pi \rightleftarrows \pi$ process is now coupled with the flipping of electrons, so that the transition has a significantly large first-order spin–orbit coupling term, resulting in a drastic enhancement of the intersystem crossing. In contrast, for the system showing minimal amount of MLCT character, the coupling between orbital and spin angular momentum should be rather small due to negligible changes of orbital angular momentum that can couple with electron flipping. In other words, the intersystem crossing can be enhanced for systems involving notable MLCT participation. Similar argument can be applied to the $T_1 \rightarrow S_0$ radiative

transition, that is, phosphorescence, in which $^3\pi\pi^*$ mixed with ^{3}MLCT states should greatly increase the transition probability, hence shorten the radiative lifetime.

DFT calculations: Realizing that the transition properties may drastically influence the photophysical behavior, assignments of electrical transitions become crucial. Empirically, this may be accomplished with the assistance of spectroscopic data. For example, allowed and partially allowed transitions may be differentiated from the associated absorption extinction coefficient, and the emission profile, such as structureless versus vibronic bands, may be exploited as a tool to assign the property of the lowest-lying triplet state. These indirect methods have proven to be too qualitative, such that erroneous assignments frequently occur. In our experience, the recently developed DFT theory provides a very accurate approach for the transition-metal complexes. The optimized structure can be obtained with either the assistance of X-ray crystal structure or geometrical optimization on the electronic ground state based on, for example, the hybrid Hartree–Fock/density functional theory (HF/DFT) method. For example, the B3LYP,[19] "double-ζ"-quality basis sets consisting of Hay and Wadt's effective core potentials (LANL2DZ)[20] are frequently employed for the transition metal elements, while the 6-31G* basis[21] is used for H, C, N, F, and O atoms. Furthermore, a relativistic effective core potential (ECP) replaces the inner core electrons of third-row Group 6 metal atoms, leaving the outer core ($5s^25p^6$) electrons and the $5d^6$ valence electrons. Time-dependent DFT (TDDFT) calculations are then performed with the same functional and basis set at the optimized geometry to obtain electronic transition energies and the associated frontier orbitals. Through the frontier orbital analyses, the type as well as percentage of orbital involving in the transition can be deduced. The calculations can be performed with the commercially available software such as the Gaussian 03 package.[22]

On the basis of the above theoretical background we hope that the interested readers can gain certain understanding on the fundamental of luminescence properties of the transition-metal complexes. This will facilitate them to catch up the core subjects regarding the choice of ligands and metals suited for enhancing emission brightness, conducting color tuning, and studies of other intriguing photophysical properties elaborated as follows.

Pyridylazolate Chromophores

The prototypical C-linked 2-pyridylazole chromophores and its derivatives are listed below, in which CF_3 or the *tert*-butyl substituent are selected according to their unique electronic properties as well as the relatively larger size so that they can provide sufficient steric shielding to the adjacent nitrogen lone-pair electrons.

The preparation of the CF_3-substituted **L1** is best executed by using a hydrazine cyclization reaction with a suitably

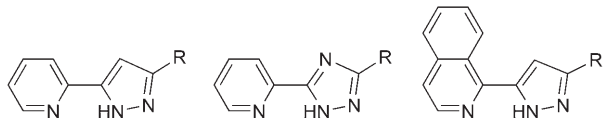

R = CF_3 (**L1**); *t*Bu (**L2**) R = CF_3 (**L3**); *t*Bu (**L4**) R = CF_3 (**L5**); *t*Bu (**L6**)

prepared pyridyl diketone intermediate, which is obtained from the base-catalyzed Claisen condensation of 2-acetyl pyridine and ethyl trifluoroacetate.[23] In contrast, preparation of *tert*-butyl-substituted **L2** can be achieved through the condensation of methyl picolinate with pinacolone, followed by treatment with anhydrous hydrazine under similar condition.[24] The isoqunioline-substituted derivatives **L5** and **L6**, which are useful for tuning the emission to longer wavelength region, were prepared from their 2-isoquinolyl reagents. Finally, C-linked 2-pyridyl-1,2,4-triazoles were synthesized according to literature methods, in which the CF_3-substituted 1,2,4-triazole **L3** was easily obtained by using 2-pyridinecarboximidamide hydrochloride and trifluoroacetic acid hydrazide; the latter is obtained by reacting ethyl trifluoroacetate with hydrazine.[25] On the other hand, the *tert*-butyl-substituted **L4** required 2-pyridinecarboxamidrazone and pivaloyl chloride in basic aqueous media, followed by dissolution of the resulting precipitate in ethylene glycol and increasing the temperature to ~210 °C.[26] Relevant chemistry dealing with the triazolate coordination compounds can be found in a number of recent review papers.[27]

Phosphorescent Metal Complexes

Organometallic complexes possessing a heavy transition-metal element are crucial for the fabrication of phosphorescent OLEDs.[28] The strong spin–orbit coupling effectively promotes intersystem crossing as well as enhances the subsequent emissive decay from the triplet excited state to the ground state (vide supra), facilitating strong phosphorescence by harvesting both singlet and triplet excitons. Because an internal quantum efficiency (η_{int}) as high as ~100% can theoretically be achieved, these heavy-metal-containing emitters are superior to their fluorescent counterparts in OLED applications.

In the following sections, the conceptual designs of the phosphorescent complexes, according to their central metal atoms, are classified into four categories, namely osmium, ruthenium, iridium, and platinum. Work emphasizing at syntheses of Os^{II}- and Ru^{II}-based materials and their utilization in OLED fabrication have been reviewed recently;[4c] however, a more general survey of second- and third-row transition metal complexes regarding their chemistry and photophysical background in this concept article would help the readers to comprehend the fundamental basis in the development of phosphorescent materials. Moreover, prototypes focused here are mainly derived from our previous work, and their extension as well as comparison with respect to

other designs will be occasionally discussed. Also, to warrant the OLED applications, neutral as opposed to the ionic complexes are the main focus here, simply due to the higher volatility and the avoidance of internal defects that were produced by the current-induced migration of ionic species.

Osmium-based emitters

Blue-emitting materials: The 2-pyridyl pyrazole ligand **L1** can readily react with boron reagent $B(C_6F_5)_3$ to form a complex with high-efficiency fluorescence in the near UV region (~380 nm).[29] This observation strongly suggests that ligands **L1**–**L4** are suitable for preparation of novel blue-emitting phosphorescent metal complexes. We then treated the pyrazole and triazole ligands **L1**, **L2**, **L3**, and **L4** with $Os_3(CO)_{12}$ at high temperature to yield the corresponding blue emitters **1**, *t*Bu-substituted **1**, **2**, and an isomeric mixture of **3** and **4**, respectively.

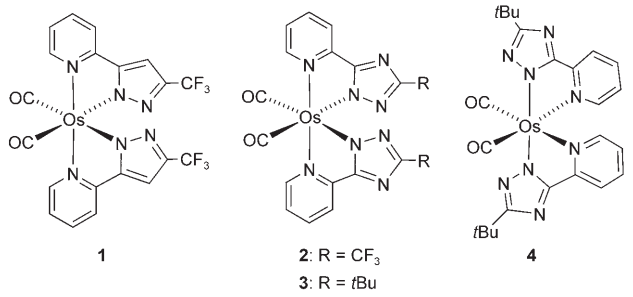

As expected, two geometrical isomers (**1**–**3** vs. **4**), both with two mutually orthogonal chelates and two *cis* CO ligands were isolated for these reactions.[29] As for the geometrical isomers **3** and **4**, Figure 1 shows the corresponding UV/Vis absorption and emission spectra in acetonitrile. Similar to the spectral data of pyrazolate complexes **1** and **2** listed in Table 1, the absorption band of **3** in the spectral region of 225–280 nm is attributed to the IL ππ* transition

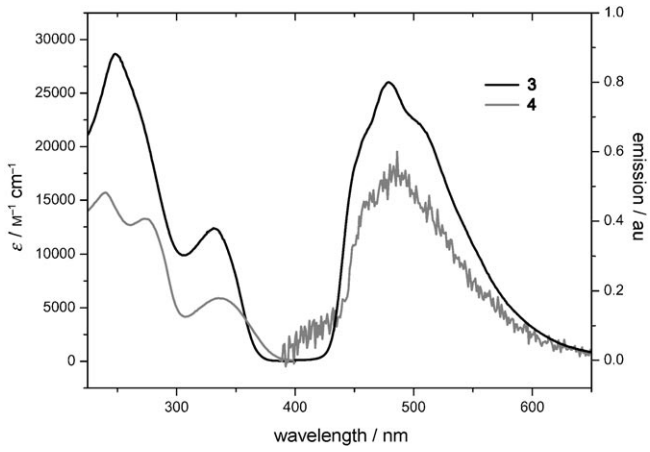

Figure 1. UV/Vis absorption and emission spectra of **3** and **4** in acetonitrile at room temperature.

Table 1. Photophysical properties of osmium complexes in degassed acetonitrile (**1**–**4**) and CH_2Cl_2 (**5**–**11**) at room temperature.[a]

	Abs. λ_{max} [nm]	λ^{em}_{max} [nm]	Φ[b]	τ_{obs} [μs]
1	311	430, 457, 480	0.14	18.5
2	307	420, 446, 468	0.23	2.9
3	333	455, 480, 507	0.42	39.9
4	340	460, 483, 515	0.00046	0.026
5	405, 454, 542	617 (618)	0.50 (0.21)	0.86 (0.63)
6	411, 456, 553	632 (655)	0.19 (0.29)	0.73 (0.61)
7	406, 466, 560	649 (670)	0.25 (0.10)	0.63 (0.44)
8	405, 457, 543	617 (631)	0.62 (0.24)	0.96 (0.18)
9	403, 457, 545	614 (618)	0.76 (0.36)	0.94 (0.58)
10	410, 465, 550	629 (634)	0.50 (0.21)	0.81 (0.91)
11	401, 448, 520	603 (613)	0.91 (0.28)	0.97 (0.14)

[a] Data in parentheses were measured in solid state at RT. [b] Quantum yield.

of the pyridine and/or triazolate fragment. The broad, structureless band maximized at 310–334 nm can be assigned to a triazolate-to-pyridine intra-ligand ππ* mixed with the ^{1}MLCT transition. Again, we like to re-emphasize here and throughout the text that the best way to access the assignment is with the help of theoretical approaches (vide supra).

Complex **3** exhibits bright blue mission ($\Phi = 0.42$) with distinct vibronic peak maxima appearing at ~455, 480, and 507 nm in degassed acetonitrile at 298 K. Its origin from the $T_1 \rightarrow S_0$ phosphorescence is verified by the drastic oxygen quenching of the emission intensity as well as the ~40 μs observed lifetime (see Table 1). Moreover, the appearance of vibronic progression warrants a dominance of the ^{3}ππ* character for the phosphorescence. In comparison, remarkable differences in emission properties were observed for **4**. Although its spectral profile looks quite similar to that of **3**, this complex is almost non-emissive at room temperature, showing quantum efficiency as low as 4.6×10^{-4} and with emission lifetime as short as 26 ns.

In our experiences, such geometry tuning photophysical behaviors are frequently encountered and have been one of our core interests amid the development of the luminescent complexes. As such, the differences between **3** and **4** provide a prototypical model to realize the indispensability of the fundamental basis in view of rationalization.

On the basis of aforementioned theory, one possibility is the existence of fast quenching processes in **4**, such as the thermal population to a MC d–d state, which results in weakening of the metal–ligand interaction due to its antibonding character and may thus act as an activator for the overall radiationless transition.[30] However, this possibility was ruled out, as none of the four lowest excited states, including two singlet and two triplet manifolds based on the DFT calculation,[31] possess the anticipated MC d–d character. The inaccessibility of the d–d excited state is believed to come from the strong ligand-field strength of the chelates as well as the CO ligands. On the other hand, the lowest-energy T_1 configuration in **4** could be reasonably attributed to a ^{3}ππ* manifold, mixed with a small amount of the ^{3}MLCT character. Thus, population of the T_1 excited state causes the shift of the electron density from the Os metal,

CO ligands, and triazolate to the pyridyl moiety, resulting in a further reduction of the already weakened Os–pyridine interactions in **4**; the latter is shown by the single-crystal X-ray analysis. As a result, the potential-energy surface of T_1 might be so shallow that, under extreme conditions, surface-crossing on potential-energy surface between S_0 and T_1 is possible. As shown in Figure 2, upon excitation, fast S_1–T_n intersystem crossing must take place. It is plausible that intersystem crossing proceeds from S_1 to T_2 due to their closeness in energy, followed by a fast rate of T_2 to T_1 internal conversion ($\leq 1\ ps^{-1}$). After population equilibrium, **4** can be thermally activated to certain vibrational levels close to the section of surface-crossing to execute the radiationless deactivation through facile metal–ligand bond stretching. Thus, a dominant $T_1 \rightarrow S_0$ radiationless transition caused by a "loose bolt" effect might take place upon thermal activation.[32]

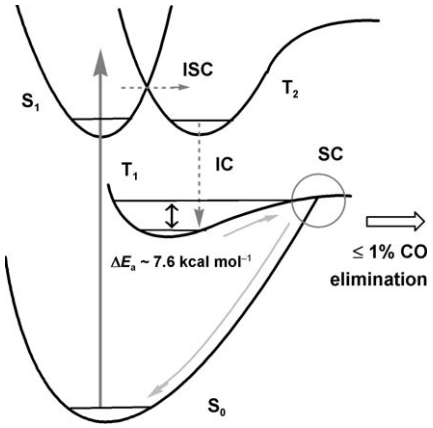

Figure 2. Energy levels of the lower-lying excited states and the proposed relaxation pathway for complex **4**. ISC: intersystem crossing, IC: internal conversion. SC: surface-crossing.

This observation allows a parallel comparison with the behavior of tris-cyclometalated iridium complexes, for which isolation of two geometrical isomers has also been documented.[33] Structural and spectroscopic data suggest that the facial isomers have the stronger and more evenly distributed metal–ligand bonding, and exhibiting bright phosphorescence in both fluid and solid states. In contrast, the meridional isomers have much greater bond length alternations caused by the differing *trans* influences of anionic phenyl and neutral nitrogen donors, such as pyridine or pyrazole, and are significantly less emissive. Naturally, this greater bond strength alternation of the meridional isomers then induces a similar "loose bolt"[32] effect upon electronic excitation, which is more likely responsible for the rapid radiationless deactivation observed in this Ir^{III} system.

Red-emitting materials: The concept of preparing red-emitting Os^{II}-based complexes can be illustrated by the exploitation of the previously discussed blue-emitting complexes **1**–**4** and their functionalized derivatives. In view of their $\pi\pi^*$ mixed with MLCT character for the lowest-lying transition, one easy way is to increase the metal-center d_π energy and concomitantly increase (decrease) the π^* energy of the ancillary ligands. This can be accomplished by replacing the strong π-accepting CO ligand by an electron-donating ligand, as well as introducing more π-electron conjugated chromophores to **1**–**4**. The desired synthesis was initiated by the treatment of respective Os^{II} complexes with Me_3NO in anhydrous diethylene glycol monoethyl ether (DGME) at 180–190 °C to eliminate the CO ligands, followed by addition of corresponding phosphane ligands.[34] A related one-pot synthetic strategy gave us the desired Os^{II} complexes **5**–**10** in much improved ($\geq 70\,\%$) yields, and hence has a great advantage in scaling up for possible industrial applications.[35]

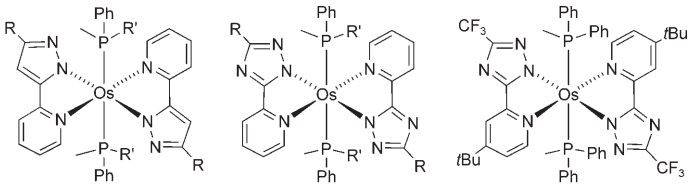

5: R = CF_3, R' = Ph
6: R = CF_3, R' = Me
7: R = *t*Bu, R' = Ph
8: R = CF_3, R' = Ph
9: R = C_3F_7, R' = Ph
10: R = C_3F_7, R' = Me
11

Figure 3 shows an ORTEP diagram of **5**, for which the metal atom is located at a crystallographic center of inversion. The two chelating pyrazolate ligands establish a nearly planar OsN_4 basal arrangement, together with two PPh_2Me

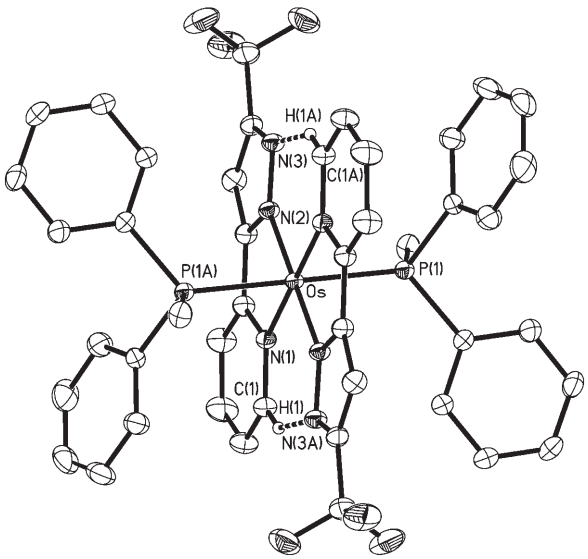

Figure 3. ORTEP diagram of **6**; selected distances: Os–P(1) = 2.3616(5), Os–N(1) = 2.090(2), Os–N(2) = 2.073(2), N(2)–N(3) = 1.349(2), N(3)···H(1A) = 2.508 Å and angles: N(1)-Os-N(2) = 76.48(7), N(1)-Os-N(2A) = 103.52(7)°.

ligands located at the *trans* positions. The planar ligand arrangement is analogous to those of the porphinato ligand in metalloporphyrins such as $[Os(ttp)(PPh_3)_2]$, ttp = *meso*-tetraphenylporphinate,[36] while a remarkable nonbonding contacts (N3A···C1 = 3.305 Å and N3 A···H1 ~ 2.50 Å) were observed between the pyridylpyrazolate chelates.

The UV/Vis spectra of all these red-emitting Os^{II} complexes showed three notable absorption maxima (Table 1). The highest-energy band, observed at ~400 nm, is assigned to the spin-allowed $^1\pi\pi^*$ transition. The next-lower energy absorption band, around 454–466 nm, can be ascribed to a spin-allowed ^{1}MLCT transition, while the third-lowest energy band can be assigned to a state involving a mixture of both $^3\pi\pi^*$ and ^{3}MLCT characters.

For the emission spectra, complex **6**, bearing $PPhMe_2$ groups, reveals a ~15 nm bathochromic shift in λ_{max} relative to the PPh_2Me-substituted derivative **5**, and can qualitatively be rationalized by an increase of the Os^{II} d_π energy level due to the poor π-accepting strength of the $PPhMe_2$ ligands (Table 1). Based on the small variation of the emission peak wavelengths between **6** (632 nm) and **10** (629 nm), or **5** (617 nm) and **8** (617 nm), we concluded that the triazolate segment exhibited only a small amount of hypsochromic displacement, although its π-accepting character should be greater than that of the pyrazolate analogue. Conversely, changing the substituent on the triazolate from *tert*-butyl to CF_3 and then to C_3F_7 caused a notable blue-shift due to the increase of MLCT gap by lowering of the metal d_π energy level, and is revealed by the notorious decrease of emission λ_{max} of complexes **7**–**9**. Finally, the observed lifetimes of ca. 0.6–0.9 μs in degassed CH_2Cl_2 are considerably shorter than those of most reported red-emitting Ir^{III} complexes, implying that the OLED devices fabricated with Os complexes could exhibit reduced triplet–triplet annihilation at higher driving voltages.[37]

These Os^{II} complexes were utilized for polymer light-emitting diodes (PLEDs), as such technologies have the potential for applications in large-area devices prepared with simple processes.[38] Preliminary electroluminescent (EL) polymer-based devices have been prepared by using poly(*N*-vinylcarbazole) (PVK) and 2-(4-biphenylyl)-5-(4-*tert*-butylphenyl)-1,3,4-oxadiazole (PBD), the latter served as electron-transporting materials to compensate for the poor electron-transporting ability of PVK.[39] Generally speaking, the energy transfer from the host polymer blend to the Os^{II} emitters is very efficient, as supported by the lack of any PVK emission in the EL spectra.

In a second study, PF-Q, a copolymer containing a polyfluorene backbone and 2,4-diphenylquinoline side chains, was used as host material and doped with 2.4 wt% of **6** to realize red EL.[40] Upon photoexcitation, the photoluminescence (PL) profile of the blend consists of two emission bands: one originates from the remaining emission of the PF-Q host, whereas the other, at about 624 nm, corresponds to the emission signal of **6**. In contrast, the host emission is quenched completely when stimulated by the EL excitation, giving red triplet emission from **6** that had Commission Internationale de L'Eclairage (CIE) color coordinates of 0.66 and 0.34 at 11 V. These results suggest that both Förster energy transfer and direct charge trapping/recombination on the Os dopant **6** are responsible for the observed EL. The much enhanced maximum external quantum efficiency of 6.63%, a luminance efficiency of 8.71 cd A^{-1}, and a brightness of 4163 cd m^{-2} were obtained at a current density of 47.8 mA cm^{-2}.

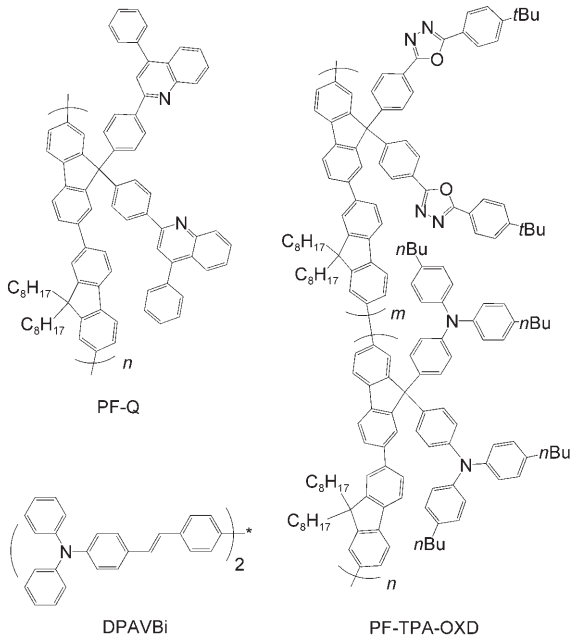

In the third approach, a tailor-made blue-emitting polyfluorene host material PF-TPA-OXD (PF = polyfluorene, TPA = triphenylamine, OXD = oxadiazole), which contains both hole- and electron-transporting side chains, has been employed in facilitating charge injection and transport, and is suitable for matching the dopant–host energy level to achieve the direct formation and confinement of an exciton at the dopant.[41] This unique design leads to a reduction in the excitation energy of the host polymer, which in turn decreases the degree of exciton loss arising from nonradiative decay of the host triplet. In practice, PLED devices with the configuration ITO/poly(styrenesulfonate)-doped poly(3,4-ethylenedioxythiophene) (PEDOT) (35 nm)/polymer emitting layer (50–70 nm) and dopant **6**/TPBI (30 nm)/Mg:Ag (100 nm)/Ag (100 nm) were fabricated, keeping the optimized dopant concentration of **6** at approximately 1 mol% (TPBI = (*N*-phenylbenzimidizol-2-yl)benzene). Again, the EL spectra indicate an exclusively dopant emission, revealing that the emission originates from the direct charge trapping, followed by recombination with opposite charges at the dopant sites.[42] For a comparison, this device reached a maximum external quantum efficiency (EQE) of 8.37% with a peak brightness of 16720 cd m^{-2}. Moreover, a maximum η_{ext} of 12.8% was achieved by using a similar device configuration, employing **6** as dopant, PF-TPA-OXD as host polymer, and PS-TPD-TFV as hole-transport layer. PS-TPD-TFV is a cross-linkable polystyrene (PS) copolymer

with both thermally curable trifluororovinyl ether (TFV) group and hole-transporting tetraphenylene biphenyldiamine (TPD) group as side branches.[43]

More recently, Shu and co-workers[44] prepared an even more interesting white-emitting PLED from compound **11** (orange), a blue-emitting distyrylarylene fluorescent dye DPAVBi, and the electron transport auxiliary PBD, co-doped into the previously mentioned PVK polymer matrix. This blended PLED exhibited an intense white emission with CIE values of 0.33 and 0.34; a high EQE of 6.12%, which corresponds to 13.2 cd A^{-1}; and a maximum brightness of 11306 cd m^{-2} at 17 V. The color hue showed little voltage-dependent variation, even at luminance as high as 1×10^4 cd m^{-2}. The excellent emission quantum efficiency, short radiative lifetime and good miscibility of **11** within the PVK blend are the key factors that gave these superior performances.

Direct vapour deposition was conducted by taking advantage of excellent volatilities and stabilities of these Os^{II} complexes.[35] Thus, complex **8** was selected as one example in fabrication of multilayer devices: ITO/HTL(40 nm)/CBP:**8**-(30 nm)/BCP(10 nm)/AlQ_3(30 nm)/LiF(1 nm)/Al(150 nm), in which CBP and BCP stand for 4,4′-*N*,*N*′-dicarbazolyl-1,1′-biphenyl and 2,9-dimethyl-4,7-diphenyl-1,10-phenanthroline, respectively. Interestingly, upon changing the hole-transport layer (HTL) from 4,49-bis[*N*-(1-naphthyl)-*N*-phenylamino]-biphenyl (NPB) to 9,9-bis{4-[di-(*p*-biphenyl)aminophenyl]}-fluorene (BPAPF), a very high initial EQE of ~20% and a luminous efficiency of 27.8 cd A^{-1} were obtained at low current density of 1 mA cm^{-2}. Taking the coupling out factor into account, this device is showing nearly 100% internal phosphorescence efficiency,[45] making them very suitable as volatile red dopants for the small molecule OLED processes.

Ruthenium-based emitters: One major obstacle to the development of phosphorescent OLED technologies lies in the prohibitive cost of the noble metals such as osmium, platinum, and even iridium. Thus, from a technological standpoint, there is an urgent need to develop phosphorescent-emitting materials that contain less expensive metals such as ruthenium.

As for a rational design suited for OLEDs, it is indispensable to have charge-neutral Ru^{II} complexes in view of volatility and charge mobility (vide supra). Secondly, the weaker ligand field strength for the second-row elements inevitably leads to the exploitation of strong bidentate ligands. Thirdly, strong field ancillary ligands, such as phosphane, are required to increase the energy gap of the MC d–d transition so that the associated radiationless deactivation can be suppressed.[46] Finally, the relatively high oxidation potential in Ru^{II} requires the employment of extensively π-conjugated chromophores, such as 1-isoquinolyl-substituted **L5** and/or **L6** to compensate the unfavorable metal oxidation potential in generation of highly efficient, saturated red emission.

Accordingly, a series of Ru^{II} complexes (**12**–**18**) were synthesized following the synthetic scheme established for their osmium counterparts.[47] The emission spectra are depicted in Figure 4, while photophysical data are listed in Table 2. In

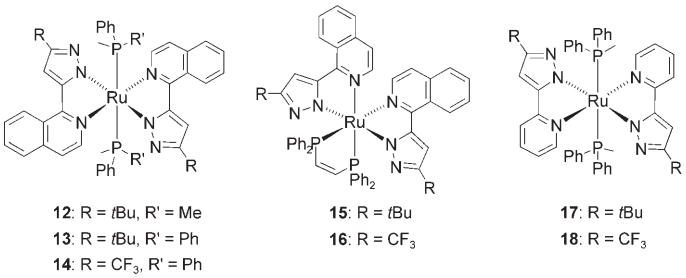

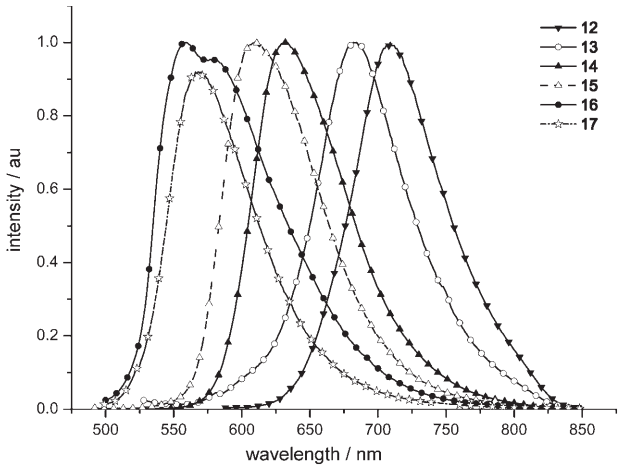

Figure 4. Photoluminescence of Ru^{II} complexes as solid film at room temperature.

good agreement with the ^{3}MLCT emission, the PPh_2Me derivative **13** exhibits a ~27 nm hypsochromic shift in λ_{max} in comparison to the $PPhMe_2$-anchored **12**, the result of which can qualitatively be rationalized by a decrease of the Ru^{II} d_π energy level due to the increase of π-accepting strength. For complex **14**, an even more notable hypsochromic shift of

Table 2. Photophysical properties of complexes **12**–**18** in CH_2Cl_2 and solid state at room temperature.

	Abs. λ_{max} [nm] ($\varepsilon\times10^3$)	λ_{max}^{em} [nm][a]	Φ[a,b]	τ_{obs} [μs][a]
12	336 (20), 363 (14), 462 (13), ~580 (0.9, br)[c]	718 (709)	– (0.02)	– (1.06)
13	332 (20), 361 (15), 455 (12), ~566 (1, br)	700 (682)	– (0.02)	– (0.64)
14	320 (25), 353 (13), 446 (17), ~523 (1, br)	636 (632)	0.01 (0.24)	0.10 (1.82)
15	316 (23), 356 (20), 368 (20), 408 (9), ~470 (4, br)	637 (609)	0.08 (0.21)	0.06 (2.1)
16	307 (22), 345 (16), 369 (18), 390 (10), ~445 (3, br)	596 (559, 581)	0.002 (0.02)	0.02 (0.56)
17	309 (19), 395 (10), 443 (1), ~493 (1, br)	– (568)	– (0.001)	– (0.16)
18	297 (22), 392 (12), ~460 (0.7, br)	–	–	–

[a] Data in parentheses were measured in solid state at RT. [b] Quantum yield. [c] br = broad.

50 nm was achieved. This is apparently caused by the electron-withdrawing effect of the CF_3 substituents on pyrazolate, which has a function of further lowering the electron density at the Ru^{II} center. Upon changing the *trans* PPh_2Me arrangement to the chelating *cis*-1,2-bis(diphenylphosphanido)ethylene, the emission underwent a further blue shift, which was revealed by the emission λ_{max} at 609 and 559 nm for **15** and **16**, respectively.[48] Moreover, the emergence of an IL $^3\pi\pi^*$ contribution for **16** is supported by the second emission peak at $\lambda_{max} = 581$ nm concluded from the observation of the vibronic coupling. This is apparently caused by the *cis*-arranged phosphane chelate, which reduced the MLCT contribution at the lowest-lying excited state. Finally, complexes **17** and **18** are essentially non-emissive at room temperature. The result is plausibly attributed to the less conjugated pyridyl groups that destabilize $\pi\pi^*$/MLCT transitions, such that the lower-lying excited states possess an increasing proportion of the MC d–d character.

As for the OLED applications, a multilayer device using 24 wt% of **14** as a dopant emitter in a CBP host and with NPB as a hole transport layer exhibits saturated red emission with an EQE of 5.10%, luminance efficiency of 5.74 cd A^{-1}, and power efficiency of 2.62 Lm W^{-1}, while incorporation of a thin layer of PEDOT/PSS between ITO and NPB optimizes the result with EQE of 7.03%, luminous efficiency of 8.02 cd A^{-1}, and power efficiency of 2.74 Lm W^{-1} at 20 mA cm^{-2}. The non-ionic nature, high-emission quantum efficiency, and short radiative lifetime are believed to be key factors for this unprecedented achievement of the Ru^{II} emitters.

Comments should be made here regarding the upper-limit of the color tuning for the Ru^{II} complexes. Unlike their third-row analogues, due to the relatively weak ligand-field strength and high oxidative potential, the MC d–d transition in the Ru^{II} complex is expected to possess a smaller energy gap and hence to appear at the lower-energy region. This should manifest the interference of MC d–d transitions in designing the Ru^{II}-based emitters particularly toward blue color. One way to push Ru^{II} complexes toward blue may lie in the use of strong π-accepting ligands such as CO. However, the net results generally cause a decrease of d_π energy without too much destabilization of the d_{σ^*} orbitals. In fact, we have experienced inferior phosphorescence efficiency once the designed ruthenium complexes reach the green-yellow emitting region.[48] Circumventing such an obstacle needs to call for certain challenging, breakthrough concepts.

Iridium-based emitters: Iridium-based emitters are considered to be the seminal generation of phosphorescence emitters. As a general approach, replacement of one cyclometalated C^N chelate in the homoleptic complex $[Ir(C^N)_3]$ with an ancillary chelate (LX) afforded heteroleptic complexes $[Ir(C^N)_2(LX)]$, in which LX = acetylacetonate (acac), *N*-methylsalicyliminate (sal), and picolinate (pic).[49] With this type of structural modification, even though the emissions retain those of their parent complexes $[Ir(C^N)_3]$, a minor dependence on the emission peak wavelength was noted, which varies according to the nature of the ancillary LX ligands. For instance, the observed emission λ_{max} of such heteroleptic complexes changes according to an order of pic < sal ~ acac, which is proportional to their electron-donor strengths, resulting in a reduction of the energy gap. Accordingly, the pyrazole ligands, such as **L1** and **L2**, and triazole ligand, such as **L3** and **L4**, were utilized to serve as the third LX ligand in conducting the color tuning. As their donor strengths are expected to follow a qualitative trend of acac ~ **L2** > **L4** ≫ **L1** > **L3**, it is not surprising to see that complexes with LX ligands **L1** or **L3** display more blue-shifted emission signals, while complexes with LX = **L2** or **L4** would give rise to red-shifted emissions relative to their parent derivative $[Ir(C^N)_3]$. Recently, the dithiolate chelates, such as *N*,*N*′-diethyldithiocarbamate (Et_2dtc) and *O*,*O*′-diethyldithiophosphate (Et_2dtp), with ligand field strengths comparable to those of the *tert*-butyl-substituted azolate, were utilized for preparation of the heteroleptic, red-emitting Ir^{III} complexes.[50]

Tuning the color to red: Cyclometalated $[Ir(ppy)_3]$ and its heteroleptic analogue such as $[Ir(ppy)_2(acac)]$ have been extensively applied in fabricating green-emitting OLED devices,[51] while the strong emission occurring at λ_{max} ~514 nm is believed to originate from the mixed triplet states possessing both IL ππ* and MLCT characters.[52] From the MO theory, it is anticipated that the LUMO and HOMO of the ppy ligand are partially located at the pyridyl part and the phenyl segment of the ppy ligand, respectively.[53] This is because that the phenyl group of ppy ligand carries a formal negative charge, and the pyridine is formally neutral. Ac-

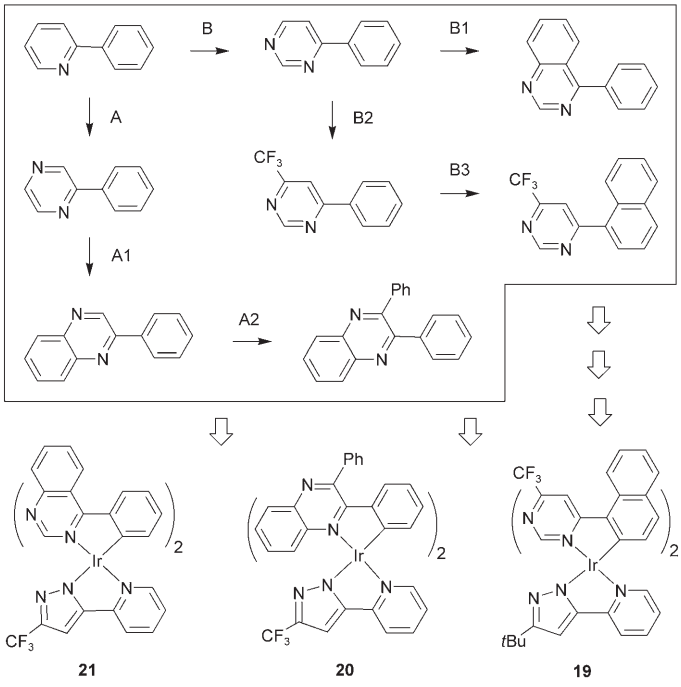

Scheme 1. Strategy for tuning the ligand emission to saturated-red and the structural drawing for relevant red-emitting iridium complexes.

cordingly, as shown in Scheme 1, replacement of one CH group at the pyridyl fragment by a nitrogen atom would give a pyrazine (step A) or a pyrimidine-substituted ligand fragment (step B), or even addition of a CF_3 group at the pyrimidine (step B2), would show a decrease in the LUMO energy level. On the other hand, the HOMO of these ligands remains unchanged, as they are mainly located at the anionic phenyl group. Thus, after formation of the Ir^{III} complexes, such a hypothetical nitrogen atom substitution at the cyclometalated ligand will cause an appreciable reduction of the energy gap for both $^3\pi\pi^*$ and ^{3}MLCT emission. This tuning strategy involving direct nitrogen-for-carbon substitution at the π-framework should be as good as or even better than the traditional method using the inductive effect of F or CF_3 substituents.[54] Further attachment of an extra aromatic hexagon into the ligand framework, for example, using quinoxaline to replace the hypothetical pyrazine fragment (step A1), quinazoline to replace pyrimidine (step B1), or even using naphthalene to replace phenyl group (step B3), should give a further decrease of the energy gap by extended π conjugation. Therefore, tuning the emission to the saturated red can be achieved using the cyclometalated ligands obtained after treating Ir^{III} complexes with steps A2, B1 and B3, together with utilization of pyridylazolate (or other chelating anions) as the third LX chelate,[55] (e.g., complexes **19**, **20** and **21**). Further tuning of emission to near-infrared (NIR) was accomplished by using a tailor-made, functionalized benzoquinoxaline chromophore.[56] Weak NIR emissions with $\lambda_{max}=910$–930 nm and $\Phi=0.022$–0.004 in aerated CH_2Cl_2 were recorded, for which the rapid radiationless deactivation may be governed by nearly temperature-independent, lower-frequency motions such as the in-plane bendings in combination with small torsional motions of accompanying phenyl substituents.

The OLED fabrication was examined by using **19** doped in a tetraphenyldiamine-based hole injection/transport layer (HTL) and poly(BTPD-Si-PFCB) as an electron-blocking and an exciton confinement layer at the anode.[57] To realize optimum efficiency, a layer of 1,3,5-tris(*N*-phenylbenzimidazol-2,yl)benzene electron-injection/transport layer (ETL) was also applied at the cathode for hole blocking and exciton confinement.[58] The device fabricated from a blended polymer involving 5 wt% of **19** in PF-TPA-OXD gave a maximum EQE of 7.9% and a maximum brightness of 15800 cd m^{-2}, with CIE chromaticity coordinates of 0.65 and 0.34.[59] These results are outstanding for red-emitting PLEDs with Ir^{III}-based dopants.

Complex **20**, which exhibited an emission λ_{max} at 640 nm, was also utilized for the preparation of PLEDs.[55] These devices consist of a multilayer configuration ITO/PEDOT:PSS/PVK-PBD (30 wt%):x wt% **20**/TPBI/Mg:Ag/Ag (100 nm) (TPBI = 2,2′,2″-(benzene-1,3,5-triyl)tris(1-phenyl-1*H*-benzimidazole)). At the doping concentration of 1.8 wt%, the device exhibited a maximum EQE of 3.15%, a brightness of 1751 cd m^{-2} at 67.4 mA cm^{-2}, and a maximum brightness of 7750 cd m^{-2} at 21 V. The performance deteriorated substantially upon increasing the doping level to 5.3 wt% of **20**, which was attributed to concentration quenching and triplet–triplet annihilation.

Preparation of OLEDs using co-evaporation was realized using complex **21**.[60] The multilayer devices of the configuration ITO/NPB (40 nm)/CBP:**21** (30 nm)/BCP (10 nm)/Alq_3 (30 nm)/Mg:Ag were prepared, with doping concentrations varying from 7, 14, and 21% up to a 100% neat film composition, for which the configuration was adopted from those reported by Thompson and Forrest.[61] Very bright emission was observed at all doping levels, among which the best performance was achieved using 14 wt% of **21**, exhibiting a maximum brightness of 12370 cd m^{-2} and an EQE of 8.1% at 20 mA cm^{-2}, but a slightly inferior CIE value of 0.62 and 0.37. It is notable that, in contrast to that of a typical phosphorescent OLED, the nondoped device employing **21** also showed electroluminescence as high as 5780 cd m^{-2}, an EQE of 5.5% at a current density of 20 mA cm^{-2}. Reduced π–π stacking in solid state and a relatively short radiative lifetime (~1 μs) has given such exceptional performances.

Blue-emitting materials: Design and preparation of high-efficiency blue-emitting phosphorescent complexes have been experiencing considerable challenges.[62] This task is far more difficult than those for preparing green and red-emitting complexes. The key lies in the selection of chelating chromophores that are suitable to form complexes with large intraligand $^3\pi\pi^*$ and/or ^{3}MLCT transition energy. To achieve the required high efficiency, attempts have been made through the use of strong-field ancillary ligands such as cyanide, CO, or even phosphane ligands with an aim to increase the HOMO–LUMO gaps.[46b,63] More recently, the blue-emitting iridium complexes with formula [$(dfppy)_2$Ir(L^X)] (dfppy = 2-(2,4-difluorophenyl) pyridine and L^X = picolinate (pic) or pyrazolyl borate ligands) were designed and synthesized in a systematic manner.[64] These results clearly demonstrate the feasibility and the methodology for obtaining blue phosphorescence.

The pyridylazolate-based ligands were found to be highly useful for such approaches. The first reported example is complex **22**,[65] which showed the blue phosphorescence with the first emission λ_{max} located at 461 nm, and exhibited a hypsochromic shift of ~10 nm versus that of Ir–picolinate derivative (FIrpic). This notable behavior is consistent with

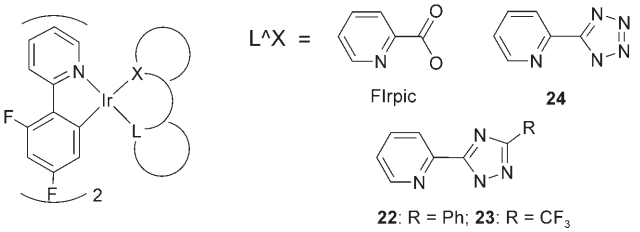

the much greater π-accepting properties of pyridyl triazolate chelate in **22** versus that of the picolinate ligand in FIrpic, further lowering the electron density at the iridium metal

center. In the case of the CF_3-substituted complex **23**, although the CF_3 group may exert a greater electron-withdrawing effect, it showed a slightly blue-shifted emission ($\lambda_{max}=459$ nm) with respect to that of **22**, while replacing the triazolate with the tetrazolate chelate ligand gave complex **24**, showing the identical emission λ_{max} at 459 nm.[66] It is interesting to note that the room-temperature emission of Os^{II} complex **2**, which is attributed to the $^3\pi\pi^*$ excited state of the triazolate ligand **L3**, occurred at the much higher energy of ~420 nm.[29] In addition, the emission of complexes **22–24** exhibits notable vibronic progression and the spectra are barely shifted when recorded at temperatures as low as 77 K. Based on these observations, the lowest-energy excited state of **22–24** must possess a mixed $^3\pi\pi^*$ and ^{3}MLCT character, in which the electron density is principally localized at the cyclometalated dfppy ligands and is thus less sensitive to the change of the pyridylazolate. A recent DFT calculation on FIrpic and derivatives showed good agreement with this delineation.[67]

The fabrication of OLEDs employing **23** and **24** and their electroluminescence characterization have been described by using a multilayer structure of ITO/NPB (30 nm)/mCP: **23** or **24** (30 nm, 7%)/TPBI(30 nm)/LiF (0.5 nm)/Al, in which mCP = 1,3-bis(9-carbazolyl) benzene.[66] It is notable that both EL spectra exhibit three vibronic shoulders at ~460, 490, and 520 nm, which are analogous to their PL spectra. However, the device that contained **24** exhibited a much more intense side band at ~490 nm that gives the CIE coordinates of 0.15 and 0.24. On the other hand, the device that contained **23** as emitter showed a significantly reduced emission shoulder at ~490 nm that allows the electroluminescence to appear in the deep-blue region with better CIE = 0.14, 0.18. When an octyl chain is introduced at the 4-position of the pyridyl group in **L3**, the resulting chelate ligand can be used to prepare analogous octyl-substituted iridium complexes for PLEDs with PVK blends.[68] The maximum brightness is 110 cd m^{-2} at 18 V, and the luminous efficiency at 100 cd m^{-2} is 0.06 cd A^{-1}, with CIE coordinates being 0.14 and 0.26.

Moreover, Chi, Chou and co-workers have also prepared a novel heteroleptic Ir^{III} complex, **25**, in an attempt to reach the so-called "true blue" phosphors.[69] It is anticipated that

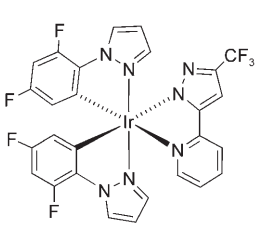

25

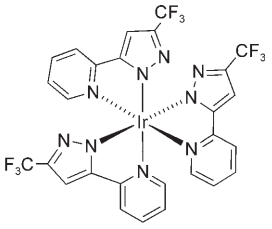

26

the dfppz ligand will display an energy gap far greater than the typical blue radiation, which was revealed by the emission envelop of [Ir(dfppz)$_3$] starting from λ_{max} ~390 nm at 77 K, (dfppz)H = 2,4-difluorophenyl pyrazole.[33] Thus, after attaching the chelate **L1** to a [Ir(dfppz)$_2$] unit giving **25**, the ligand $\pi\pi^*$ character of **L1** should dominate the excited state manifolds, showing the required blue phosphorescence with an additional ~30 nm blue shift relative to those of complexes **22–24** (Figure 5). This is indeed what had occurred; however, the emission quantum yield turned out to be rather low ($\Phi=0.007$) in solution, making this molecular

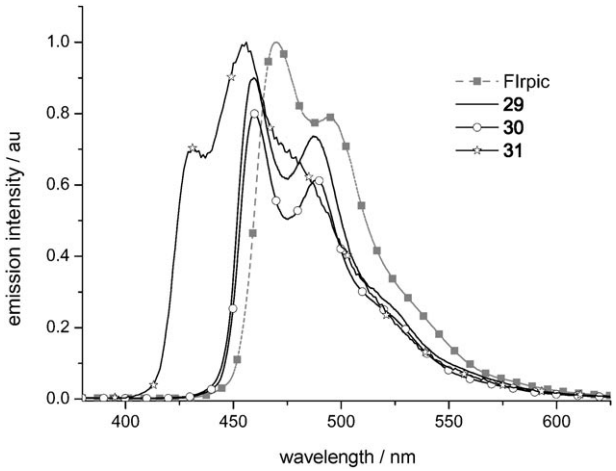

Figure 5. Photoluminescence of iridium phosphors at room temperature in CH_2Cl_2.

design somewhat useless for fabricating of blue OLEDs. The DFT calculation on **25** has again ruled out the MC d–d transition to be the dominant deactivation process. Alternatively, we speculate that, because the triplet states are in a high-energy blue region, it would display a relatively shallow potential-energy surface and may allow a fast surface-crossing to the ground state. Although detailed insights into the deactivation mechanism are still pending, the experimentally extracted activation energy of 4.43 kcal mol^{-1} (~1550 cm^{-1}) of a related complex provides an estimate of the T_1–S_0 gap at the surface-crossing section, while the pre-exponential factor of 1.25×10^{12} s^{-1} reflects the vibrational frequency of the weakly bonding modes channelling into the major radiationless pathway.

More recently, meridional Ir^{III} complexes with three pyridylazolate ligands were also successfully synthesized.[70] The spectral data of **26** and its triazolate analogues demonstrate an unprecedented dual phosphorescence, that is, blue (P_1) and green (P_2) bands deriving from the intraligand and ligand-to-ligand charge transfer states, T_{ILCT} and T_{LLCT}, respectively. The fast decay of the blue phosphorescence (430 nm in **26**) at room temperature is attributed to the rapid conversion from T_{ILCT} to T_{LLCT} states, for which the T_{ILCT} and T_{LLCT} states are nearly orthogonal to each other and possessing mainly the ligand $\pi\pi^*$ character together with a small extent (~10%) and an enhanced (20%) MLCT character, respectively. The T_{ILCT} state is preferentially populated after vertical (Franck Condon) excitation at RT,

as estimated by TD-DFT calculation. Subsequently, $T_{ILCT} \rightarrow T_{LLCT}$ transfer takes place with an energy barrier (~ 6.9 kcal mol^{-1}) possibly due to certain large-amplitude motions and bring out the weak T_{LLCT} emission (P_2, 530 nm). On the other hand, the T_{LLCT} population was expected to decrease upon lowering the temperature, which then make the $T_{ILCT} \rightarrow S_0$ transition (the P_1 band) as the dominant decay process. This scenario, involving the rapid conversion from triplet T_{ILCT} to T_{LLCT} states as depicted in Figure 6, has also been supported by steady-state kinetics and the theoretical approach.

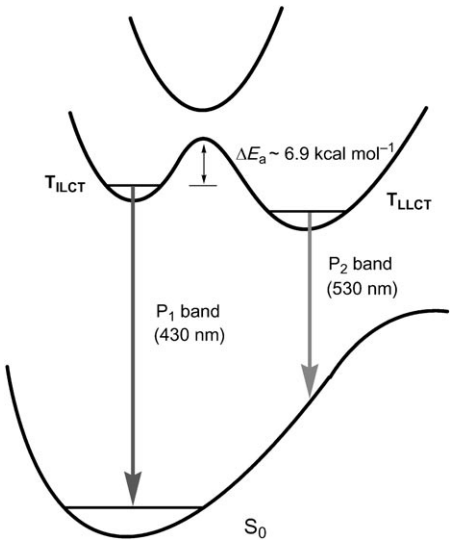

Figure 6. The proposed mechanism for the dual phosphorescence in **26**.

Platinum-based emitters: Many Pt^{II} complexes were evaluated as the potential dopants or emitters for OLEDs.[71] Particularly, Pt^{II}–porphyrin complexes were the first and most promising deep-red light-emitting dyes, despite their large structural diversity found in the synthesized porphyrin frameworks.[72] Furthermore, utilization of cyclometalated ligands or multidentate chelates or Schiff base ligands allowed the successful preparation of yellow-, green-, and even white-emitting OLEDs.[4b,73]

It is notable that the square-planar geometry of Pt^{II} complexes allows formation of dimer, excimer, and even aggregate through axial coordination, resulting in distinctively different photophysical properties when compared to the previously discussed, d^6 octahedral metal complexes.[74] Thus, in addition to the typical MLCT and ligand-centered $\pi\pi^*$ transition that occurred in the d^6 complexes, a new type of electronic transition, denoted as metal-metal-to-ligand charge transfer (MMLCT), became possible; this type of transfer involves a charge transfer between the filled Pt–Pt bonding orbital and a vacant, ligand-based π^* molecular orbital.[75] The pyridylazolate-based Pt^{II} complexes showed no exception from such behavior, and their photophysical properties will be elaborated by systematically changing the ligand design.

These pyridylazolate-based Pt^{II} complexes can be obtained via treatment of the in-situ-generated pyridylazolate anion with $[PtCl_2(dmso)_2]$ in THF, or through a direct combination of the respective azoles with K_2PtCl_4 in refluxing ethanol.[76] Both methods gave the anticipated products in good yields, and four representative molecular drawings are depicted below.

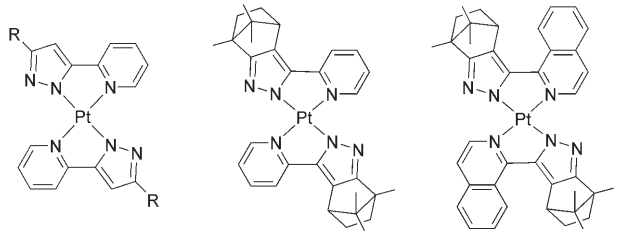

27: R = *t*Bu; **28**: R=CF_3 **29** **30**

As depicted in Figure 7, for the first complex **27**, the lower-lying absorption bands at 416 nm are assigned to the transition incorporating a state mixing singlet and triplet MLCT transitions and, to a certain extent, the intraligand $^3\pi\pi^*$ transitions. The strong singlet–triplet mixing is confirmed by the significant overlap between the UV/Vis absorption bands and the leading edge of the respective emission peak profile. Moreover, its emission occurred at 494 nm ($\Phi = 0.19$; $\tau = 0.4$ μs) in degassed THF.

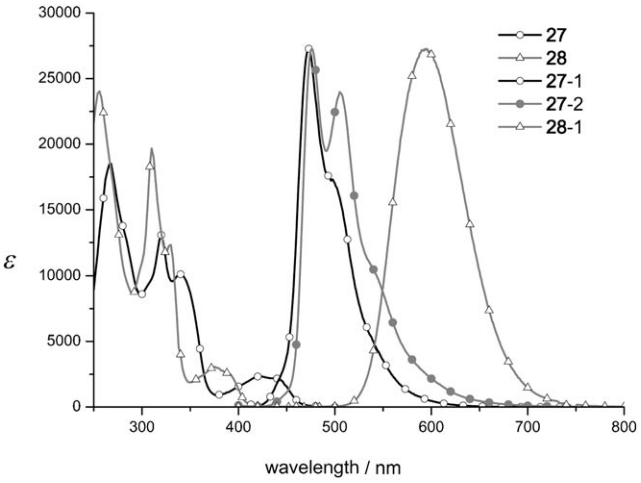

Figure 7. The UV/Vis and emission spectra of **27** and **28** in CH_2Cl_2; emission spectrum **27**-1 was recorded in CH_2Cl_2, while emission spectra **27**-2 and **28**-1 were recorded as thin film samples.

Intriguingly, the absorption and solid-state emission spectra of the second of Pt^{II} complex **28** are distinctively different. Significant blue shift of the MLCT absorption was noted in their UV/Vis absorption spectra. The increase in energy gap of MLCT transitions is apparently caused by the electron-withdrawing effect of CF_3 substituents, which induce an increase of the π^* acidity of the azolate and lower

the Pt^{II} metal 5d energy level. Concomitantly, the higher-energy ππ* transitions, which are located at the UV region, also display a similar hypsochromic shift due to the increase of the IL ππ* energy gap.[77] In sharp contrast, the solid-state emission occurred at the much lower-energy position compared to that of **27**. As a result, the featureless solid-state emissions observed are assigned to the MMLCT transition,[78] which is in sharp contrast to that of the emission profile of **27** in the solid state, showing three distinct vibronic peaks, a feature indicates the increased amount of ^{3}ππ* character. The poor solubility of **28** in almost all organic solvents confirms their high tendency to form aggregation, for which the linear stacking arrangement with short Pt–Pt separation of 3.442 Å was confirmed by single-crystal X-ray diffraction study on its C_3F_7 analogue.[76]

Moreover, the achievement of high luminescence efficiency for pyridylazolate-based Pt^{II} complexes was realized by constructing a skeleton that greatly suppresses the aggregation effect. A rigid blocker, such as the camphor-derived functionality, was then incorporated into the above-mentioned Pt^{II} complexes to reduce the aggregation and suppress ^{3}MMLCT transitions.[79] As such, these complexes showed unprecedented bright phosphorescence (e.g. **29**: $\lambda_{max}=553$ nm; $\Phi=0.64$ and **30**: $\lambda_{max}=635$ nm; $\Phi=0.81$) in degassed CH_2Cl_2 solution at RT.

OLED devices fabricated using **30** as a dopant emitter has been achieved in the multilayer configuration of ITO/NPB/CBP: **30**/BCP/AlQ_3/LiF/Al. At a dopant concentration of 12%, the device gave a bright red emission with λ_{max} at 612 nm and a very high EQE of ~7% at a driving current of 20 mA. Upon increasing the doping level to 100%, electroluminescence peaked at 630 nm, EQE = 3.2%, and a luminance efficiency of 3.5 cd A^{-1}, and a power efficiency of 1.52 Lm W^{-1} was achieved at 20 mA.[79] The reduced red shift (18 nm) for the 100% doped device confirmed the nonexistence of aggregation for **30** in the solid state.

Concluding Remarks

This research concept of transition-metal-based "phosphorescence dyes" offers immense opportunity toward applications, particularly on the urgent need in OLEDs. Bearing this goal in mind, in this concept article, we have presented both the design of their molecular architectures stemmed from their fundamental bases, and the succinct theoretical background suited for depicting their excitation behaviors. We also bring out a critical issue in that the photophysical properties, such as lower-lying electronic transitions, the radiative lifetime, and the possible radiationless deactivation processes, can be rationalized. As systematic analyses have been accumulated and formulated accordingly; those properties may even be predicted in a qualitative manner, saving a great deal of trial-and-error synthetic efforts.

As for the ligand selection, it is remarkable that the pyridylazolate-based ligands can react with a variety of metal elements, covering second-row element Ru^{II} and third-row elements such as Os^{II}, Ir^{III}, and Pt^{II}, to form various neutral, stable and highly luminous coordination complexes. We also demonstrate the power of merging theoretical and experimental measurement of a new series of luminescent complexes in rational way. A broad spectrum of color ranging from blue to red has been achieved by derivatization of pyridylazolate ligands as well as by variation of the electronic properties of the central metal through adjusting the ancillary ligands. Particular attention should be drawn to the Ru^{II} complexes **12**–**14** for their potential capability to lower the cost of OLED materials. In the case of neutral Ru^{II} complexes, we trust that the strategy for averting the incorporation of MC d–d character into the lowest triplet state should be equally applicable to other systems involving second-row transition metal elements. Last but not the least, one pending challenge lies in achieving the efficient blue-emitting phosphors, the success for which greatly demands ingenious, creative concepts grounded by the fundamental basis.

In view of applications, we have provided several examples toward making all types of OLEDs with excellent performance. On the one hand, it is possible that these pyridylazolate-based metal complexes, after full optimization, will eventually find certain industrial applications in the development of OLED devices. On the other hand, the results as well as the perspectives of our studies should spark a continuous interest in the design and preparation of other luminescent materials incorporating both main-group and transition-metal elements and for the development of inorganic and organometallic photochemistry. For example, on the basis of a similar principle, we believe that coarse- as well as fine-tuning of emission toward near-IR region with high luminescent efficiency is feasible, rendering their future applications in other arenas such as solar cell and near-IR imaging, and so forth. We thus believe that this article should provide a useful conceptual guide, on the platform of OLEDs, to both nonspecialist readers and experts with a new angle on a familiar problem.

Acknowledgements

The authors are grateful for financial supports from both the National Science Council and the Ministry of Economy. We also thank all of our co-workers whose names are listed in our publications.

[1] a) A. Juris, V. Balzani, F. Barigelletti, S. Campagna, P. Belser, A. von Zelewsky, *Coord. Chem. Rev.* **1988**, *84*, 85; b) E. C. Constable, P. J. Steel, *Coord. Chem. Rev.* **1989**, *93*, 205; c) V. Balzani, A. Juris, *Coord. Chem. Rev.* **2001**, *211*, 97; d) S. Serroni, S. Campagna, F. Puntoriero, C. Di Pietro, N. D. McClenaghan, F. Loiseau, *Chem. Soc. Rev.* **2001**, *30*, 367.

[2] a) M. G. Colombo, A. Hauser, H. U. Güdel, *Top. Curr. Chem.* **1994**, *171*, 143; b) K. P. Balashev, M. V. Puzyk, V. S. Kotlyar, M. V. Kulikova, *Coord. Chem. Rev.* **1997**, *159*, 109; c) B. Ma, P. I. Djurovich, M. E. Thompson, *Coord. Chem. Rev.* **2005**, *249*, 1501.

[3] a) J. A. Treadway, B. Loeb, R. Lopez, P. A. Anderson, F. R. Keene, T. J. Meyer, *Inorg. Chem.* **1996**, *35*, 2242; b) C. N. Fleming, K. A. Maxwell, J. M. DeSimone, T. J. Meyer, J. M. Papanikolas, *J. Am. Chem. Soc.* **2001**, *123*, 10336; c) S. Chardon-Noblat, A. Deronzier, F.

Hartl, J. Van Slageren, T. Mahabiersing, *Eur. J. Inorg. Chem.* **2001**, 613.
[4] a) E. Holder, B. M. W. Langeveld, U. S. Schubert, *Adv. Mater.* **2005**, *17*, 1109; b) J. Brooks, Y. Babayan, S. Lamansky, P. I. Djurovich, I. Tsyba, R. Bau, M. E. Thompson, *Inorg. Chem.* **2002**, *41*, 3055; c) P. T. Chou, Y. Chi, *Eur. J. Inorg. Chem.* **2006**, 3319.
[5] a) J. C. Jeffery, P. L. Jones, K. L. V. Mann, E. Psillakis, J. A. McCleverty, M. D. Ward, C. M. White, *Chem. Commun.* **1997**, 175; b) A. Chadghan, J. Pons, A. Caubet, J. Casabo, J. Ros, A. Alvarez-Larena, J. F. Piniella, *Polyhedron* **2000**, *19*, 855.
[6] E. M. Tjiou, A. Fruchier, V. Pellegrin, G. Tarrago, *J. Heterocycl. Chem.* **1989**, *26*, 893.
[7] a) R. Hage, J. G. Haasnoot, J. Reedijk, J. G. Vos, *Chemtracts: Inorg. Chem.* **1992**, *4*, 75; b) R. Hage, J. G. Haasnoot, J. Reedijk, R. Wang, J. G. Vos, *Inorg. Chem.* **1991**, *30*, 3263.
[8] a) Y. C. Adachi, R. C. Kwong, P. Djurovich, V. Adamovich, M. A. Baldo, M. E. Thompson, S. R. Forrest, *Appl. Phys. Lett.* **2001**, *79*, 2082; b) X. Jiang, A. K.-Y. Jen, B. Carlson, L. R. Dalton, *Appl. Phys. Lett.* **2002**, *80*, 713.
[9] R. C. Evans, P. Douglas, C. J. Winscom, *Coord. Chem. Rev.* **2006**, *250*, 2093.
[10] A. J. Lees, *Chem. Rev.* **1987**, *87*, 711.
[11] A. Vlcek, Jr., *Coord. Chem. Rev.* **1998**, *177*, 219.
[12] a) A. Vlcek, Jr., *Coord. Chem. Rev.* **2002**, *230*, 225; b) W. F. Fu, R. van Eldik, *Inorg. Chem.* **1998**, *37*, 1044.
[13] a) N. J. Lundin, A. G. Blackman, K. C. Gordon, D. L. Officer, *Angew. Chem.* **2006**, *118*, 2644; *Angew. Chem. Int. Ed.* **2006**, *45*, 2582; b) S. Ranjan, S.-Y. Lin, K.-C. Hwang, Y. Chi, W.-L. Ching, C.-S. Liu, Y.-T. Tao, C.-H. Chien, S.-M. Peng, G.-H. Lee, *Inorg. Chem.* **2003**, *42*, 1248.
[14] a) V. A. Montes, R. Pohl, J. Shinar, P. J. Anzenbacher, *Chem. Eur. J.* **2006**, *12*, 4523; b) G. Yu, S. Yin, Y. Liu, Z. Shuai, D. Zhu, *J. Am. Chem. Soc.* **2003**, *125*, 14816.
[15] a) S. Paulson, B. P. Sullivan, J. V. Caspar, *J. Am. Chem. Soc.* **1992**, *114*, 6905; b) D. S. William, A. V. Korolev, *Inorg. Chem.* **1998**, *37*, 3809.
[16] a) P. C. Ford, A. Vogler, *Acc. Chem. Res.* **1993**, *26*, 220; b) V. W.-W. Yam, K. K.-W. Lo, *Chem. Soc. Rev.* **1999**, *28*, 323.
[17] Y. G. Ma, C.-M. Che, H.-Y. Chao, X. M. Zhou, W.-H. Chan, J. C. Shen, *Adv. Mater.* **1999**, *11*, 852.
[18] T. Yutaka, S. Obara, S. Ogawa, K. Nozaki, N. Ikeda, T. Ohno, Y. Ishii, K. Sakai, M. Haga, *Inorg. Chem.* **2005**, *44*, 4737.
[19] a) A. D. Becke, *J. Chem. Phys.* **1993**, *98*, 5648; b) C. Lee, W. Yang, R. G. Parr, *Phys. Rev. B* **1988**, *37*, 785.
[20] a) P. J. Hay, W. R. Wadt, *J. Chem. Phys.* **1985**, *82*, 270; b) W. R. Wadt, P. J. Hay, *J. Chem. Phys.* **1985**, *82*, 284; c) P. J. Hay, W. R. Wadt, *J. Chem. Phys.* **1985**, *82*, 299.
[21] P. C. Hariharan, J. A. Pople, *Mol. Phys.* **1974**, *27*, 209.
[22] Gaussian 03, Revision C.02, M. J. Frisch, G. W. Trucks, H. B. Schlegel, G. E. Scuseria, M. A. Robb, J. R. Cheeseman, Jr., J. A. Montgomery, T. Vreven, K. N. Kudin, J. C. Burant, J. M. Millam, S. S. Iyengar, J. Tomasi, V. Barone, B. Mennucci, M. Cossi, G. Scalmani, N. Rega, G. A. Petersson, H. Nakatsuji, M. Hada, M. Ehara, K. Toyota, R. Fukuda, J. Hasegawa, M. Ishida, T. Nakajima, Y. Honda, O. Kitao, H. Nakai, M. Klene, X. Li, J. E. Knox, H. P. Hratchian, J. B. Cross, V. Bakken, C. Adamo, J. Jaramillo, R. Gomperts, R. E. Stratmann, O. Yazyev, A. J. Austin, R. Cammi, C. Pomelli, J. W. Ochterski, P. Y. Ayala, K. Morokuma, G. A. Voth, P. Salvador, J. J. Dannenberg, V. G. Zakrzewski, S. Dapprich, A. D. Daniels, M. C. Strain, O. Farkas, D. K. Malick, A. D. Rabuck, K. Raghavachari, J. B. Foresman, J. V. Ortiz, Q. Cui, A. G. Baboul, S. Clifford, J. Cioslowski, B. B. Stefanov, G. Liu, A. Liashenko, P. Piskorz, I. Komaromi, R. L. Martin, D. J. Fox, T. Keith, M. A. Al-Laham, C. Y. Peng, A. Nanayakkara, M. Challacombe, P. M. W. Gill, B. Johnson, W. Chen, M. W. Wong, C. Gonzalez, J. A. Pople, Gaussian, Inc., Wallingford CT, **2004**.
[23] a) S. P. Singh, D. Kumar, B. G. Jones, M. D. Threadgill, *J. Fluorine Chem.* **1999**, *94*, 199; b) W. R. Thiel, J. Eppinger, *Chem. Eur. J.* **1997**, *3*, 696.
[24] A. Satake, T. Nakata, *J. Am. Chem. Soc.* **1998**, *120*, 10391.
[25] K. Funabiki, N. Noma, G. Kuzuya, M. Matsui, K. Shibata, *J. Chem. Res. Miniprint* **1999**, 1301.
[26] a) R. Hage, R. Prins, J. G. Haasnoot, J. Reedijk, J. G. Vos, *J. Chem. Soc. Dalton Trans.* **1987**, 1387; b) P. M. Hergenrother, *J. Heterocycl. Chem.* **1969**, *6*, 965; c) S. Kubota, M. Uda, T. Nakagawa, *J. Heterocycl. Chem.* **1975**, *12*, 855.
[27] a) R. Hage, *Coord. Chem. Rev.* **1991**, *111*, 161; b) T. E. Keyes, C. M. O'Connor, J. G. Vos, *Chem. Commun.* **1998**, 889; c) J. G. Haasnoot, *Coord. Chem. Rev.* **2000**, *200–202*, 131.
[28] a) M. A. Baldo, D. F. O'Brien, Y. You, A. Shoustikov, S. Sibley, M. E. Thompson, S. R. Forrest, *Nature* **1998**, *395*, 151; b) M. A. Baldo, M. E. Thompson, S. R. Forrest, *Pure Appl. Chem.* **1999**, *71*, 2095.
[29] a) P.-C. Wu, J.-K. Yu, Y.-H. Song, Y. Chi, P.-T. Chou, S.-M. Peng, G.-H. Lee, *Organometallics* **2003**, *22*, 4938; b) J.-K. Yu, Y.-H. Hu, Y.-M. Cheng, P.-T. Chou, S.-M. Peng, G.-H. Lee, A. J. Carty, Y.-L. Tung, S.-W. Lee, Y. Chi, C.-S. Liu, *Chem. Eur. J.* **2004**, *10*, 6255.
[30] a) A. Vogler, H. Kunkely, *Top. Curr. Chem.* **2001**, *213*, 143; b) M. M. Glezen, A. J. Lees, *J. Am. Chem. Soc.* **1988**, *110*, 3892.
[31] P. J. Hay, *J. Phys. Chem. A* **2002**, *106*, 1634.
[32] N. J. Turro, *Modern Molecular Photochemistry*, **1991**, University Science Books, Mill Valley, California, Chapter 6, p. 170.
[33] a) A. B. Tamayo, B. D. Alleyne, P. I. Djurovich, S. Lamansky, I. Tsyba, N. N. Ho, R. Bau, M. E. Thompson, *J. Am. Chem. Soc.* **2003**, *125*, 7377; b) T. Karatsu, T. Nakamura, S. Yagai, A. Kitamura, K. Yamaguchi, Y. Matsushima, T. Iwata, Y. Hori, T. Hagiwara, *Chem. Lett.* **2003**, *32*, 886.
[34] Y.-L. Tung, P.-C. Wu, C.-S. Liu, Y. Chi, J.-K. Yu, Y.-H. Hu, P.-T. Chou, S.-M. Peng, G.-H. Lee, Y. Tao, A. J. Carty, C.-F. Shu, F.-I. Wu, *Organometallics* **2004**, *23*, 3745.
[35] Y.-L. Tung, S.-W. Lee, Y. Chi, Y.-T. Tao, C.-H. Chien, Y.-M. Cheng, P.-T. Chou, S.-M. Peng, C.-S. Liu, *J. Mater. Chem.* **2005**, *15*, 460.
[36] C. M. Che, T. F. Lai, W. C. Chung, W. P. Schaefer, H. B. Gray, *Inorg. Chem.* **1987**, *26*, 3907.
[37] F.-I. Wu, P.-I. Shih, C.-F. Shu, Y.-L. Tung, Y. Chi, *Macromolecules* **2005**, *38*, 9028.
[38] J. Lu, Y. Tao, Y. Chi, Y.-L. Tung, *Synth. Met.* **2005**, *155*, 56.
[39] a) X. Yang, D. Neher, D. Hertel, T. K. Daubler, *Adv. Mater.* **2004**, *16*, 161; b) C. Jiang, W. Yang, J. Peng, S. Xiao, Y. Cao, *Adv. Mater.* **2004**, *16*, 537.
[40] H.-J. Su, F.-I. Wu, C.-F. Shu, Y.-L. Tung, Y. Chi, G.-H. Lee, *J. Polym. Sci. Part A* **2005**, *43*, 859.
[41] F.-I. Wu, P.-I. Shih, Y.-H. Tseng, G.-Y. Chen, C.-H. Chien, C.-F. Shu, Y.-L. Tung, Y. Chi, A. K.-Y. Jen, *J. Phys. Chem. B* **2005**, *109*, 14000.
[42] a) M. Uchida, C. Adachi, T. Koyama, Y. Taniguchi, *J. Appl. Phys.* **1999**, *86*, 1680; b) F.-C. Chen, S. C. Chang, G. He, S. Pyo, Y. Yang, M. Kurotaki, J. Kido, *J. Polym. Sci. Part B* **2003**, *41*, 2681.
[43] Y.-H. Niu, Y.-L. Tung, Y. Chi, C.-F. Shu, J. H. Kim, B. Chen, J. Luo, A. J. Carty, A. K.-Y. Jen, *Chem. Mater.* **2005**, *17*, 3532.
[44] P.-I. Shih, C.-F. Shu, Y.-L. Tung, Y. Chi, *Appl. Phys. Lett.* **2006**, *88*, 251110.
[45] a) C. Adachi, M. A. Baldo, M. E. Thompson, S. R. Forrest, *J. Appl. Phys.* **2001**, *90*, 5048; b) M. Ikai, S. Tokito, Y. Sakamoto, T. Suzuki, Y. Taga, *Appl. Phys. Lett.* **2001**, *79*, 156.
[46] a) S. Zalis, I. R. Farrell, A. Vlcek, *J. Am. Chem. Soc.* **2003**, *125*, 4580; b) M. K. Nazeeruddin, R. Humphry-Baker, D. Berner, S. Rivier, L. Zuppiroli, M. Graetzel, *J. Am. Chem. Soc.* **2003**, *125*, 8790.
[47] Y.-L. Tung, S.-W. Lee, Y. Chi, L.-S. Chen, C.-F. Shu, F.-I. Wu, A. J. Carty, P.-T. Chou, S.-M. Peng, G.-H. Lee, *Adv. Mater.* **2005**, *17*, 1059.
[48] Y.-L. Tung, L.-S. Chen, Y. Chi, P.-T. Chou, Y.-M. Cheng, E. Y. Li, G.-H. Lee, C.-F. Shu, F.-I. Wu, A. J. Carty, *Adv. Funct. Mater.* **2006**, *16*, 1615.
[49] a) S. Lamansky, P. Djurovich, D. Murphy, F. Abdel-Razzaq, H.-E. Lee, C. Adachi, P. E. Burrows, S. R. Forrest, M. E. Thompson, *J. Am. Chem. Soc.* **2001**, *123*, 4304; b) S. Lamansky, P. Djurovich, D. Murphy, F. Abdel-Razzaq, R. Kwong, I. Tsyba, M. Bortz, B. Mui, R. Bau, M. E. Thompson, *Inorg. Chem.* **2001**, *40*, 1704.

[50] L. Chen, H. You, C. Yang, X. Zhang, J. Qin, D. Ma, *J. Mater. Chem.* **2006**, *16*, 3332.
[51] a) M. A. Baldo, S. Lamansky, P. E. Burrows, M. E. Thompson, S. R. Forrest, *Appl. Phys. Lett.* **1999**, *75*, 4; b) D. Bruce, M. M. Richter, *Anal. Chem.* **2002**, *74*, 1340.
[52] a) S. Sprouse, K. A. King, P. J. Spellane, R. J. Watts, *J. Am. Chem. Soc.* **1984**, *106*, 6647; b) A. P. Wilde, K. A. King, R. J. Watts, *J. Phys. Chem.* **1991**, *95*, 629; c) M. G. Colombo, T. C. Brunold, T. Riedener, H. U. Guedel, M. Fortsch, H.-B. Buergi, *Inorg. Chem.* **1994**, *33*, 545.
[53] H.-Y. Chen, Y. Chi, C.-S. Liu, J.-K. Yu, Y.-M. Cheng, K.-S. Chen, P.-T. Chou, S.-M. Peng, G.-H. Lee, A. J. Carty, S.-J. Yeh, C.-T. Chen, *Adv. Funct. Mater.* **2005**, *15*, 567.
[54] M. S. Lowry, S. Bernhard, *Chem. Eur. J.* **2006**, *12*, 7970.
[55] F.-M. Hwang, H.-Y. Chen, P.-S. Chen, C.-S. Liu, Y. Chi, C.-F. Shu, F.-I. Wu, P.-T. Chou, S.-M. Peng, G.-H. Lee, *Inorg. Chem.* **2005**, *44*, 1344.
[56] H.-Y. Chen, C.-H. Yang, Y. Chi, Y.-M. Cheng, Y.-S. Yeh, P.-T. Chou, H.-Y. Hsieh, C.-S. Liu, S.-M. Peng, G.-H. Lee, *Can. J. Chem.* **2006**, *84*, 309.
[57] X. Jiang, S. Liu, M. S. Liu, P. Herguth, A. K.-Y. Jen, H. Fong, M. Sarikaya, *Adv. Funct. Mater.* **2002**, *12*, 745.
[58] Y. Li, M. K. Fung, Z. Xie, S.-T. Lee, L.-S. Hung, J. Shi, *Adv. Mater.* **2002**, *14*, 1317.
[59] Y.-H. Niu, B. Chen, S. Liu, H. Yip, J. Bardecker, A. K.-Y. Jen, J. Kavitha, Y. Chi, C.-F. Shu, Y.-H. Tseng, C.-H. Chien, *Appl. Phys. Lett.* **2004**, *85*, 1619.
[60] Y.-H. Song, S.-J. Yeh, C.-T. Chen, Y. Chi, C.-S. Liu, J.-K. Yu, Y.-H. Hu, P.-T. Chou, S.-M. Peng, G.-H. Lee, *Adv. Funct. Mater.* **2004**, *14*, 1221.
[61] C. Adachi, M. A. Baldo, S. R. Forrest, M. E. Thompson, *Appl. Phys. Lett.* **2000**, *77*, 904.
[62] a) X. Ren, J. Li, R. J. Holmes, P. I. Djurovich, S. R. Forrest, M. E. Thompson, *Chem. Mater.* **2004**, *16*, 4743; b) S. Tokito, T. Iijima, Y. Suzuri, H. Kita, T. Tsuzuki, F. Sato, *Appl. Phys. Lett.* **2003**, *83*, 569; c) R. J. Holmes, B. W. D'Andrade, S. R. Forrest, X. Ren, J. Li, M. E. Thompson, *Appl. Phys. Lett.* **2003**, *83*, 3818.
[63] a) C.-L. Lee, R. R. Das, J.-J. Kim, *Chem. Mater.* **2004**, *16*, 4642; b) Y.-Y. Lyu, Y. Byun, O. Kwon, E. Han, W. S. Jeon, R. R. Das, K. Char, *J. Phys. Chem. B* **2006**, *110*, 10303.
[64] J. Li, P. I. Djurovich, B. D. Alleyne, M. Yousufuddin, N. N. Ho, J. C. Thomas, J. C. Peters, R. Bau, M. E. Thompson, *Inorg. Chem.* **2005**, *44*, 1713.
[65] P. Coppo, E. A. Plummer, L. De Cola, *Chem. Commun.* **2004**, 1774.
[66] S.-J. Yeh, W.-C. Wu, C.-T. Chen, Y.-H. Song, Y. Chi, M.-H. Ho, S.-F. Hsu, C.-H. Chen, *Adv. Mater.* **2005**, *17*, 285.
[67] Y. You, S. Y. Park, *J. Am. Chem. Soc.* **2005**, *127*, 12438.
[68] C. S. K. Mak, A. Hayer, S. I. Pascu, S. E. Watkins, A. B. Holmes, A. Koehler, R. H. Friend, *Chem. Commun.* **2005**, 4708.
[69] C.-H. Yang, S.-W. Li, Y. Chi, Y.-M. Cheng, Y.-S. Yeh, P.-T. Chou, G.-H. Lee, C.-H. Wang, C.-F. Shu, *Inorg. Chem.* **2005**, *44*, 7770.
[70] Y.-S. Yeh, Y.-M. Cheng, P.-T. Chou, G.-H. Lee, C.-H. Yang, Y. Chi, C.-H. Wang, *ChemPhysChem* **2006**, *7*, 2294.
[71] a) A. S. Ionkin, W. J. Marshall, Y. Wang, *Organometallics* **2005**, *24*, 619; b) P. T. Furuta, L. Deng, S. Garon, M. E. Thompson, J. M. J. Frechet, *J. Am. Chem. Soc.* **2004**, *126*, 15388; c) W. Sotoyama, T. Satoh, N. Sawatari, H. Inoue, *Appl. Phys. Lett.* **2005**, *86*, 153505.
[72] a) C.-M. Che, Y.-J. Hou, M. C. W. Chan, J. Guo, Y. Liu, Y. Wang, *J. Mater. Chem.* **2003**, *13*, 1362; b) Q. Hou, Y. Zhang, F. Li, J. Peng, Y. Cao, *Organometallics* **2005**, *24*, 4509; c) M. Ikai, F. Ishikawa, N. Aratani, A. Osuka, S. Kawabata, T. Kajioka, H. Takeuchi, H. Fujikawa, Y. Taga, *Adv. Funct. Mater.* **2006**, *16*, 515.
[73] a) Y.-Y. Lin, S.-C. Chan, M. C. W. Chan, Y.-J. Hou, N. Zhu, C.-M. Che, Y. Liu, Y. Wang, *Chem. Eur. J.* **2003**, *9*, 1263; b) C.-M. Che, S.-C. Chan, H.-F. Xiang, M. C. W. Chan, Y. Liu, Y. Wang, *Chem. Commun.* **2004**, 1484; c) C.-C. Kwok, H. M. Y. Ngai, S.-C. Chan, I. H. T. Sham, C.-M. Che, N. Zhu, *Inorg. Chem.* **2005**, *44*, 4442; d) W.-Y. Wong, Z. He, S.-K. So, K.-L. Tong, Z. Lin, *Organometallics* **2005**, *24*, 4079; e) F. Galbrecht, X. H. Yang, B. S. Nehls, D. Neher, T. Farrell, U. Scherf, *Chem. Commun.* **2005**, 2378.
[74] B. Ma, J. Li, P. I. Djurovich, M. Yousufuddin, R. Bau, M. E. Thompson, *J. Am. Chem. Soc.* **2005**, *127*, 28.
[75] S.-W. Lai, C.-M. Che, *Top. Curr. Chem.* **2004**, *241*, 27.
[76] S.-Y. Chang, J. Kavitha, S.-W. Li, C.-S. Hsu, Y. Chi, Y.-S. Yeh, P.-T. Chou, G.-H. Lee, A. J. Carty, Y.-T. Tao, C.-H. Chien, *Inorg. Chem.* **2006**, *45*, 137.
[77] C.-C. Cheng, W.-S. Yu, P.-T. Chou, S.-M. Peng, G.-H. Lee, P.-C. Wu, Y.-H. Song, Y. Chi, *Chem. Commun.* **2003**, 2628.
[78] a) V. H. Houlding, V. M. Miskowski, *Coord. Chem. Rev.* **1991**, *111*, 145; b) H. Yersin, U. Riedl, *Inorg. Chem.* **1995**, *34*, 1642.
[79] J. Kavitha, S.-Y. Chang, Y. Chi, J.-K. Yu, Y.-H. Hu, P.-T. Chou, S.-M. Peng, G.-H. Lee, Y.-T. Tao, C.-H. Chien, A. J. Carty, *Adv. Funct. Mater.* **2005**, *15*, 223.

Published online: December 5, 2006

